ADVENTURES IN CRYSTAL ENGINEERING†

Edward R. T. Tiekink

Department of Chemistry, National University of Singapore, Singapore 117543

†This paper is based on a lecture presented at the Eleventh Slovenian-Croatian Crystallographic Meeting held at Bohinj, Slovenia during June 27-30th, 2002

Received 05-01-2003

Abstract

An overview of the structural systematics of four heavy-element systems is given, namely triorganotincarboxylates ($R_3Sn(O_2CR')$), zinc and mercury xanthates ($A(S_2COR)_2$; A = Zn and Hg) and bismuth xanthates ($Bi(S_2COR)_3$). It will be demonstrated that there exists a fascinating range of structural diversity for these compounds, including differences in coordination number and molecular geometry. Difference in structure in two of the systems, *i.e*. $R_3Sn(O_2CR')$ and $Zn(S_2COR)_2$, are correlated with the nature of the tin- and ligand-bound R groups, respectively. This suggests a new design concept for crystal engineering, *i.e.* steric control over molecular aggregation. However, this concept is shown not to be universal by an analysis of the related $Hg(S_2COR)_2$ structures. The adoption of different motifs for $Bi(S_2COR)_3$ influences the nature of generated nanoparticles and thereby demonstrates the importance of structure of the precursor material. Finally, an example of the utility of non-traditional intermolecular 'aurophilic' (*i.e*. Au…Au) interactions upon polymer formation is demonstrated for a pair of phosphinegold(I) thiolate structures.

1. Introduction

A new field is gaining prominence in chemistry/materials science, namely *crystal engineering*. Whereas synthetic chemists have traditionally concerned themselves with the formation of intra-atomic connectivities leading to the formation of molecules, the crystal engineer is more concerned with arranging, in a specific pattern, these molecular entities in the crystalline state. The importance of this new endeavor may be ascertained by the fact that both society, *i.e*. American Chemical Society (*Crystal Growth & Design*[1]) and Royal Society of Chemistry (*CrystEngComm*[2]), and commercial, *i.e.* Elsevier Science (*Crystal Engineering*[3]), publishers have established new Journals to report advances in this area. Putting the aesthetic appeal of crystal engineering to one side, the primary motivation for work in this area relates to the generation of materials with different properties (*e.g*. electronic, optic, catalytic, magnetic, *etc*.) compared with the individual molecules (*synthons* or *tectons*) from which they are constructed. The tools available to the crystal engineer, over and beyond design concept, are

intermolecular forces in all of their guises. An obvious choice, given their strength and directionality, are hydrogen-bonding interactions involving atoms such as oxygen and nitrogen. In this context, the crystal engineer may also try to exploit the hydrogen-bonding acceptor potential of halides and less electronegative elements such as sulfur and selenium. In addition to these, there are π…π as well as C-H…π interactions available in the engineer's toolbox. In metal-containing systems, hypervalent interactions between the metal and electronegative elements such as oxygen come into play. These secondary interactions can become quite significant if the Lewis acidity of the metal center is sufficiently great. Interactions of this type form the focus of the present discussion that will primarily describe some crystal chemistry of tin, zinc, bismuth and mercury. A case will be put forward in which steric control, exerted by metal- or ligand-bound R substituents, over molecular aggregation can be achieved, at least for some systems. In the same way, a nice example of tuning intermolecular interactions, *i.e.* hydrogen-bonding *vs* aurophilic (*i.e.* Au…Au) interactions, will be described for some phosphinegold(I) systems.

2. Steric control of molecular aggregation in some main group element systems

2.1 Organotin carboxylates

Organotin carboxylates, *i.e.* compounds with the general formula $R_{4-n}Sn(O_2CR')_n$ for R and R' = alkyl and aryl, form a very important class of compounds owing to their applications in areas as diverse as agriculture, catalysis and, potentially, medicine.[4,5] Amongst the most important of these are the triorganotin carboxylates, *i.e.* $R_3Sn(O_2CR')$, and therefore it is not surprising that these have been subjected to a large number of X-ray crystal structure determinations. In fact, approximately 150 structures are available in the literature. Systematic surveys of their solid state structures[6-8] have revealed that there are four clearly defined structural motifs for these compounds as illustrated in Scheme 1. The simplest of these motifs is that shown in Scheme 1(a). This motif is monomeric and features a monodentate or, more commonly, an asymmetrically coordinating carboxylate ligand. Thus, coordination geometries may range from approximately tetrahedral to distorted trigonal bipyramidal depending upon the strength of the weaker O→Sn interaction. It is important to realize in the context of the following discussion that the weaker of the oxygen to tin interactions is indeed a

hypervalent interaction. In a formal sense, tin has its valency satisfied by four bonds, in this case provided by one oxygen and three carbon atoms. The additional interaction is therefore over and above the requirements of valency. Of course this is a formalism but, important to realize in terms of the structural variability found for the $R_3Sn(O_2CR')$ structures. The three remaining motifs feature some sort of molecular aggregation.

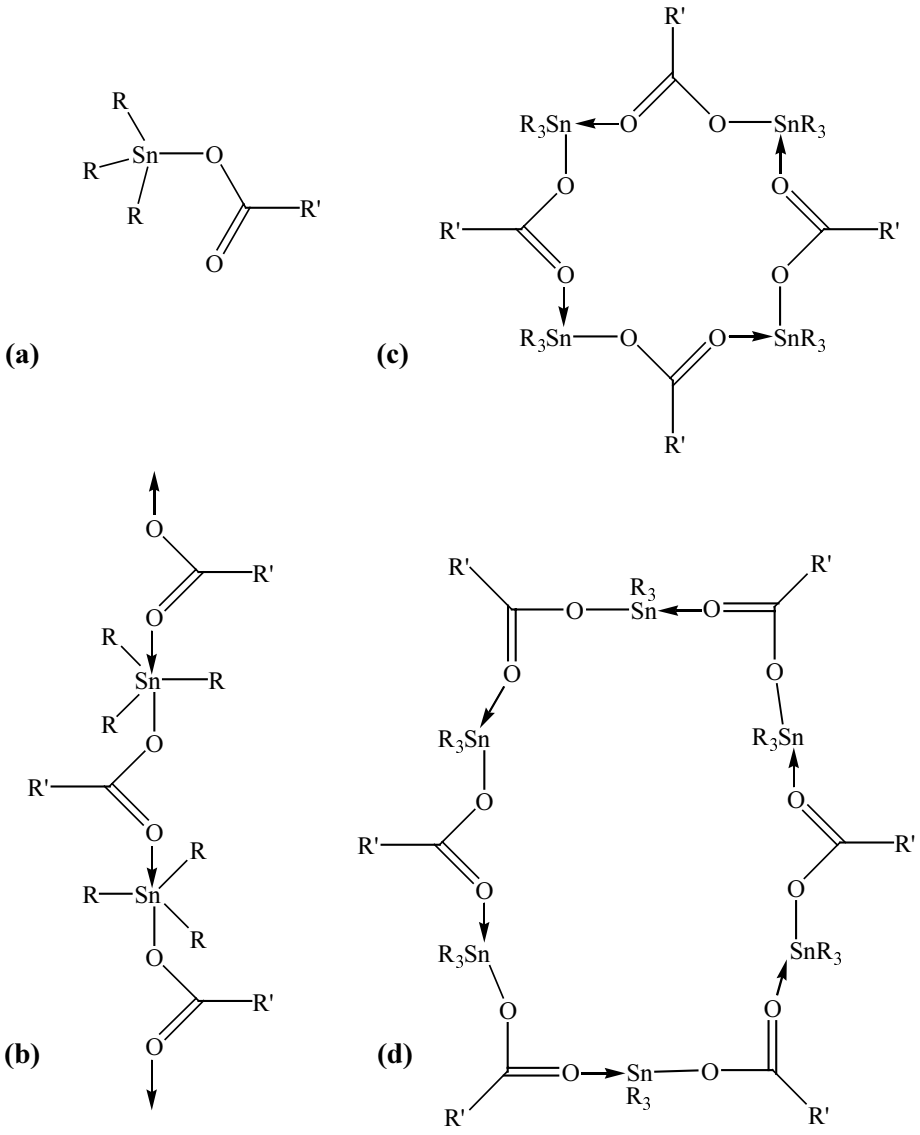

Scheme 1. Different structural motifs observed for structures of the general formula $R_3Sn(O_2CR')$ for R, R' = alkyl and aryl.

In the second motif, shown in Scheme 1(b), the monomeric entities of motif (a) aggregate *via* intermolecular O→Sn interactions leading to the formation of polymeric

chains in which the tin atoms exist in distorted *trans*-C_3SnO_2 coordination geometries. This geometry is also found in the remaining motifs that feature reduced intermolecular aggregation. The motifs illustrated in Schemes 1(c) and (d) are oligomeric, being tetrameric and hexameric, respectively. Rather than forming the linear polymeric chain, the entities cyclize into ring structures. It turns out that each of the last two motifs is adopted by one compound only and therefore, these must be considered as 'oddities'. The overwhelming majority of the structurally characterized compounds adopt one of motifs (a) and (b). Despite the relatively large number of structures of the general formula $R_3Sn(O_2CR')$ that are available in the literature, there is a dearth of *systematic* analyses. While this is unfortunate, it must be appreciated that such studies are predicated upon the availability of suitable crystals.

One system that did provide a number of crystals suitable for a systematic analysis was that containing the anion derived from the carboxylic acid shown in Scheme 2, *i.e.* 2-[(*E*)-2-(2-hydroxy-5-methylphenyl)-1-diazenyl]benzoic acid.

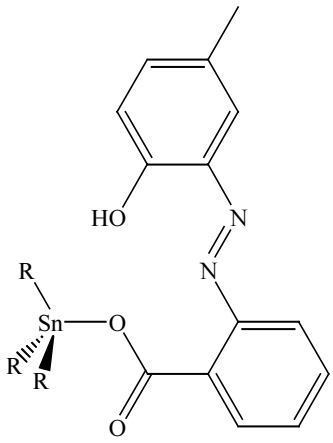

Scheme 2. The chemical structure of $R_3Sn(O_2CR^1)$ where HO_2CR^1 is the carboxylic acid $HO_2CC_6H_4N{=}NC_6H_3$-2-OH-5-Me and R = Me, Et, nBu, Ph and c-Hex.

Thus, suitable crystals for X-ray structural analysis were obtained for $R_3Sn(O_2CC_6H_4N{=}NC_6H_3$-2-OH-5-Me) with R = Me, Et, nBu, Ph and c-Hex.[8] The molecular structure of the R = c-Hex derivative is shown in Figure 1(a). Clearly, this compound adopts motif (a) as shown in Scheme 1(a) with a coordination geometry based on a tetrahedron. The R = Ph compound is in essential agreement with this structure. By contrast to these monomeric structures, polymeric structures are found for the R =

Me, Et and nBu derivatives as illustrated in Figure 1(b) for the R = Me compound. This structure conforms to motif (b) and features the expected trigonal bipyramidal geometry.

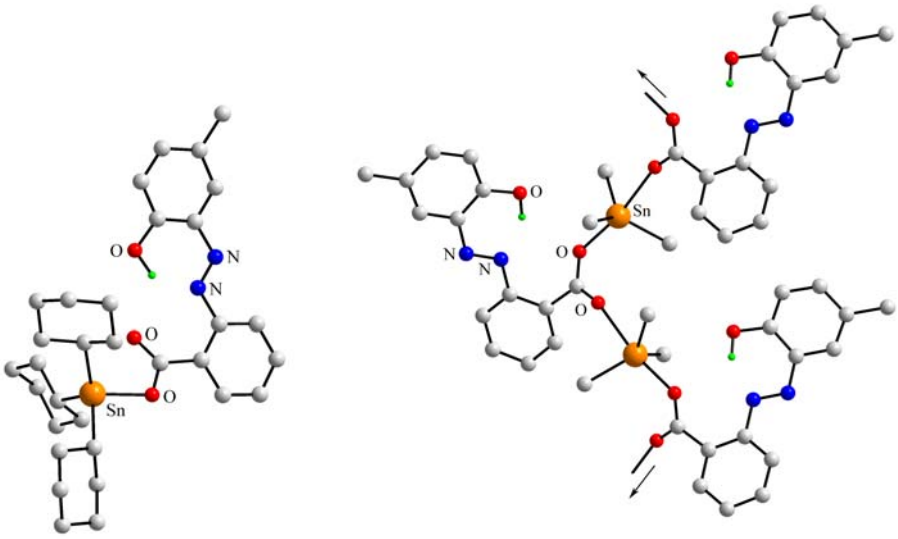

Figure 1. (a) The molecular structure of mononuclear (c-Hex)$_3$Sn($O_2CC_6H_4N$=NC_6H_3-2-OH-5-Me); and (b) The polymeric structure of [$Me_3Sn(O_2CC_6H_4N$=NC_6H_3-2-OH-5-Me)]$_\infty$. Carbon-bound hydrogen atoms have been removed for clarity.

The question is: why are such distinct motifs found for these compounds? The answer lies in a detailed analysis of their crystal structures. It had already been highlighted in the literature by Ng *et al.*[9] that the repeat distance in the polymeric $R_3Sn(O_2CR')$ structures was remarkably invariant at 5.19 ± 0.21 Å, regardless of the nature of the R and R' groups. The repeat distance calculated for the R = Me, Et and nBu structures in the present series of 4.89, 5.20 and 5.03 Å, respectively are consistent with the analysis conducted by Ng *et al.*[9] The key to understanding the structural diversity in this system was to determine the analogous repeat distance for the monomeric structures. These were 4.75 and 5.17 Å for the R = Ph and c-Hex structures, respectively, values that fall within the range determined for the polymeric motif. Figure 2 shows two strands of representative crystal structures, *i.e.* of R = Me and c-Hex. From this Figure and considering the above 'repeat' distances, a process of crystallization may be envisaged. Before continuing it is necessary to highlight one most important set of experiments. These were solution state tin-119 NMR measurements which revealed that

whatever the nature of the tin-bound R group, the molecules were dissociated, *i.e.* monomeric, in solution. Therefore, any association between molecules observed crystallographically is due to solid state effects. In the crystallization process, one can imagine the regular deposition of molecules so as to form crystals. In the case of the R = Me compound, adjacent molecules assume positions to maximize their intermolecular associations, a fundamental precept of stable solids, and, accordingly, form intermolecular O→Sn interactions leading to the formation of the polymeric motif (b). By contrast, for the R = c-Hex molecules, the steric bulk of the tin-bound groups precludes such intermolecular O→Sn associations and hence, monomeric species are found in the solid state. In the case of the R = Me compound, the hypervalent O→Sn interactions are intermolecular whereas these are intramolecular for the R = c-Hex compound. This study shows the possibility of controlling the formation of one motif over another by simply varying the steric profile of the Lewis acidic tin centers. This

(a)

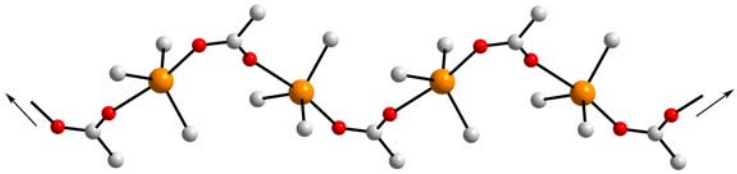

(b)

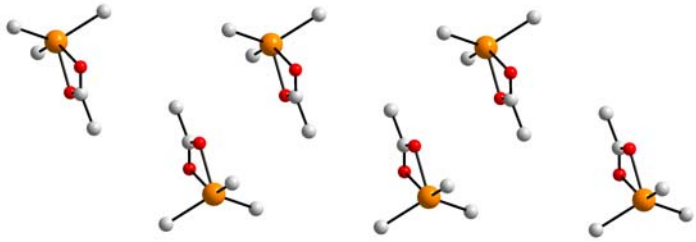

Figure 2. Packing patterns for $R_3Sn(O_2CC_6H_4N{=}NC_6H_3$-2-OH-5-Me): (a) R = Me for which the repeat distance is approximately 4.9 Å; (b) R = c-Hex for which the Sn…Sn separation between successive tin atoms is approximately 5.1 Å. Only the tin, tin-bound carbon and O_2CC atoms are shown for clarity.

principle is, in essence, akin to that which states that high coordination numbers may be obtained with small (and electronegative) donors such as fluoride and low coordination numbers generated with bulky substituents such as 2,6-diphenylphenoxide. However, in

the case of the organotin compounds, the principle is extended to intermolecular aggregation. In the next section, the possibility of extending of this principle of steric control over molecular aggregation to zinc thiolates is explored.

2.2 Zinc xanthates

In this section the structures of three xanthate structures of zinc(II) are described and in the next, those of the analogous mercury(II) xanthates. The zinc-triad 1,1-dithiolates form an important class of compounds with varied applications such as vulcanization agents, wear inhibitors, precursors for nanoparticles, *etc*. As a consequence, their structural chemistry has received considerable attention over the years and these studies provide a fascinating range of structural motifs, some of which are described here in **2.2** and later in **2.4**.

The chemical structure for $Zn(S_2COR)_2$ is misleading as it has no relevance to the observed structures, at least as determined by X-ray crystallography, owing to considerable molecular aggregation in the solid state. Indeed, three quite distinct motifs are found as the nature of the remote R substituent of the xanthate ligand is varied. In this system, the valency of the central element is satisfied by two bonds. Despite this, hypervalent Zn…S interactions lead to significant intermolecular aggregation and distorted tetrahedral geometries for zinc.

The molecular structure of $[Zn(S_2COiPr)_2]_4$[10] is shown in Figure 3(a). This compound is tetrameric in the solid state and comprises isolated 16-membered rings. In this description, four zinc atoms define the corners of a square with each edge spanned by a bidentate bridging xanthate ligand. Each of the remaining xanthate ligands chelates a zinc center and in this way may be thought as occupying terminal positions as no bridges to adjacent tetrameric units are found. The 16-membered ring is a common feature of the zinc xanthates and is found in the remaining two motifs.

The second motif for $Zn(S_2COR)_2$ is illustrated in Figure 3(b) and is found for the R = nPr[11] derivative in which both bridging and chelating xanthate ligands are present. The 16-membered rings are now corner-shared in this motif as opposed to the isolated tetrameric motif described above. Thus, the structure forms a chain but, links between chains are precluded by the presence of the 'terminal' chelating xanthate ligands. In the final motif, represented in Figure 3(c) for $[Zn(S_2COEt)_2]_\infty$,[12] all xanthate ligands are

bridging leading to a 2-dimensional or layer structure comprised of interconnected 16-membered rings.

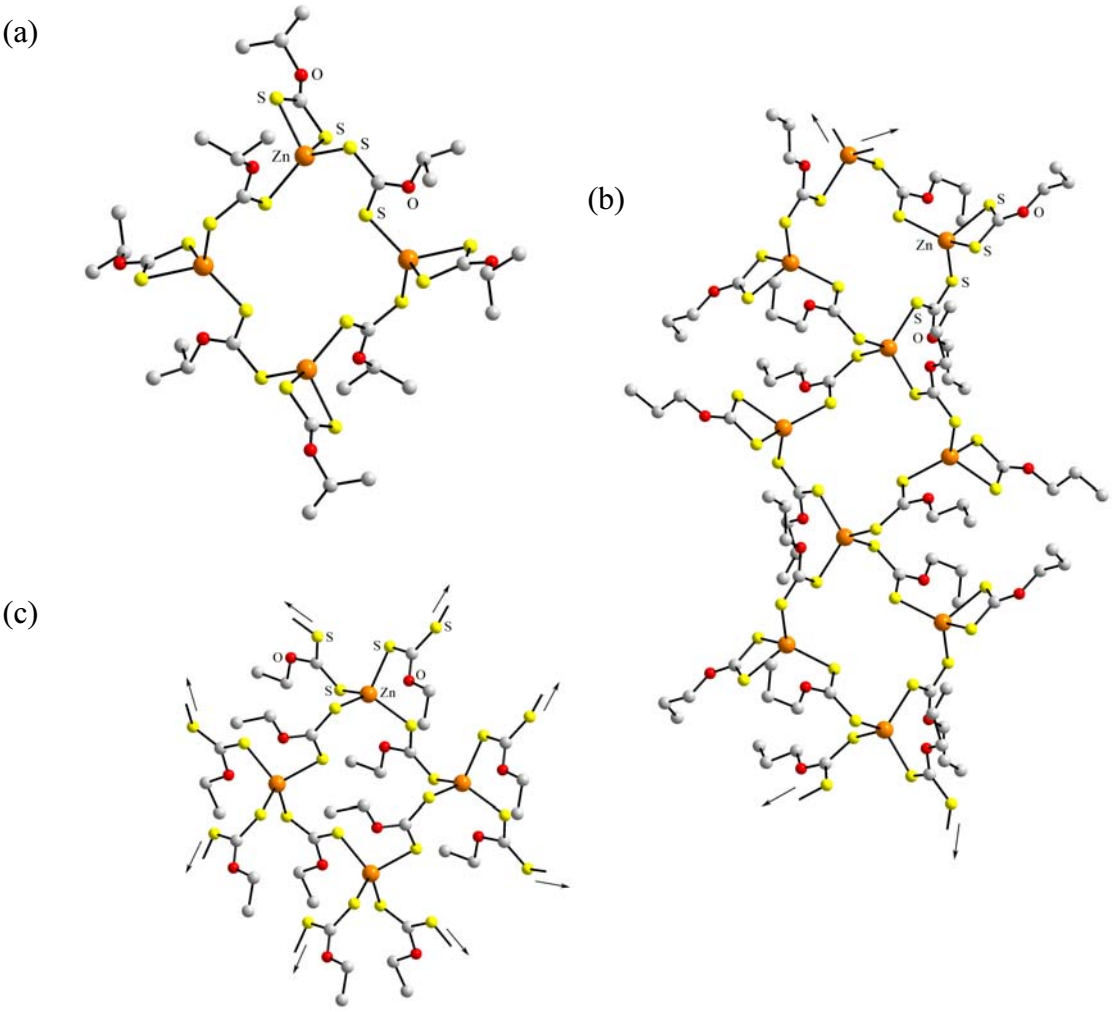

Figure 3. (a) The tetrameric structure of $[Zn(S_2COiPr)_2]_4$; (b) The chain structure of $[Zn(S_2COnPr)_2]_\infty$; and (c) The 2-dimensional structure of $[Zn(S_2COEt)_2]_\infty$. Carbon-bound hydrogen atoms have been omitted for clarity.

The first point to take note of is the remarkable structural diversity as the R group in $Zn(S_2COR)_2$ is altered. Systematic structural[13,14] and theoretical studies[15] show that there are no chemical reasons associated with the xanthate ligand to account for such structural diversity pointing to crystal packing considerations as the important determining factor. Indeed, a qualitative explanation, based upon the steric

considerations may be put forward to rationalize the appearance of the different structures observed in the solid state. Increased molecular aggregation, *i.e.* from isolated tetrameric to a chain to a layer motif in the zinc xanthates, is correlated with the decreased steric profile of the xanthate-bound R group, *i.e.* R = iPr, nPr and Et. In this way, the 'steric' principle established above for the $R_3Sn(O_2CR')$ structures is carried forward into the zinc xanthates. Further, an 'attractive' story of crystal engineering can be delineated for these compounds.

Taking the tetrameric structure found for $[Zn(S_2COiPr)_2]_4$ as a starting point, and defining this as a molecular paving stone, Figure 4(a), one can convert this into a row of paving stones when R is changed to nPr, Figure 4(b). Finally, by having R = Et, an architecture is constructed, a paved floor, Figure 4(c).

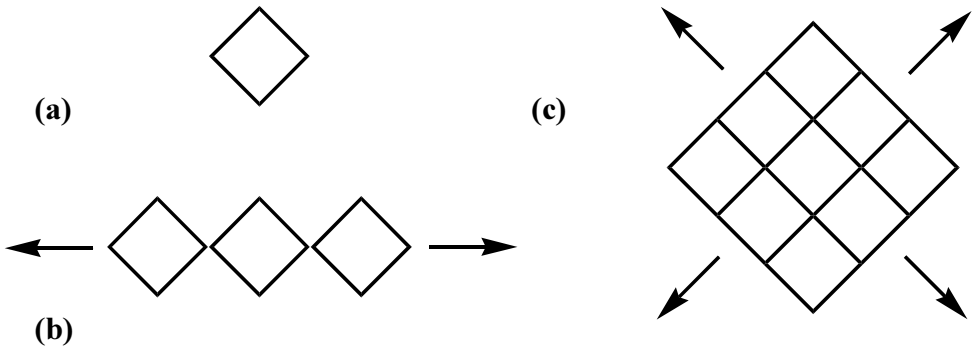

Figure 4. A crystal engineering story for $Zn(S_2COR)_2$. (a) A paving stone for R = iPr, (b) A row of pavers for R = nPr, and (c) A pathway for R = Et.

Arguably, the above is an example of the aesthetic appeal of crystal engineering. In the *Introduction*, it was stated that the main driving force behind crystal engineering was the generation of materials with different properties from their molecular precursors. Then, the question must be posed: are the different structures established for the zinc xanthates of any importance/relevance in terms of materials science. The short answer is that this has yet to be explored fully. Despite the fact that widely different motifs are found for $Zn(S_2COR)_2$, their controlled thermal decomposition invariably leads to the formation of the cubic form of ZnS (*i.e.* sphalerite) but other applications/properties have not been investigated. However, room for optimism in this context is found in the closely related bismuth xanthates, $Bi(S_2COR)_3$, for which it has been demonstrated that

there is an influence of precursor molecular architecture and the formation of Bi_2S_3 nanoparticles generated from them.

2.3 Bismuth xanthates

Two distinct structural motifs are known for the bismuth xanthates. Most of the structures conform to the dimeric structure illustrated in Figure 5(a). Here, two molecules of $Bi(S_2COR)_3$ associate, normally, about a center of inversion, *via* intermolecular (hypervalent) S→Bi interactions. The bismuth atom is 7-coordinate and all xanthate ligands are chelating but, with somewhat asymmetric Bi−S bond distances. The second motif, shown in Figure 5(b), is polymeric as a result of one of the xanthate ligands being tridentate, chelating one bismuth atom while at the same linking a

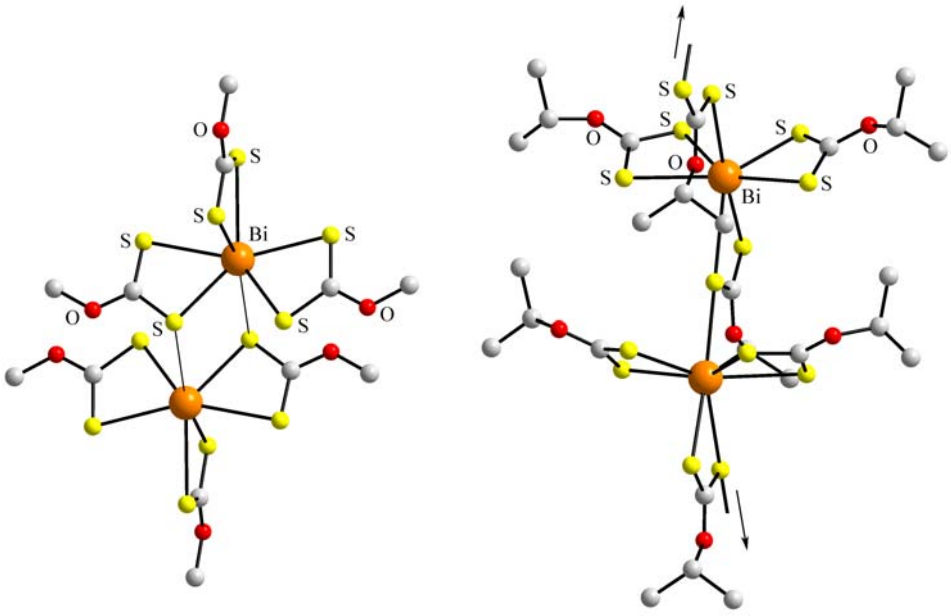

(a) (b)

Figure 5. (a) The dimeric structure of $[Bi(S_2COMe)_3]_2$; (b) The polymeric structure of $[Bi(S_2COiPr)_3]_\infty$. Carbon-bound hydrogen atoms have been omitted for clarity.

neighboring bismuth atom. The bismuth atom is again 7-coordinate. The dimeric motif is found for R = Me[16] and Et,[17] and the polymeric motif is found for R = iPr.[18] Related to the question posed for the zinc xanthates in **2.2**, *i.e.* are the different structures

relevant to materials chemistry, in the case of the bismuth xanthates, a study of their solvothermal decomposition and chemical vapor deposition of Bi_2S_3 using these precursors has been conducted.[19]

The study alluded to above showed that the nature of the precursor structural motif does indeed exert an influence upon the formation of the Bi_2S_3 nanocomposites generated. As an example, in Figure 6, scanning electron microscopy (SEM) photographs of Bi_2S_3 thin films generated from the chemical vapor deposition of (a) $[Bi(S_2COEt)_3]_2$ and (b) $[Bi(S_2COiPr)_3]_\infty$ precursor materials clearly show differences in that nanorods (20 x 150 nm) are generated by the former (as well as by $[Bi(S_2COMe)_3]_2$) but micro-sized crystals are obtained using $[Bi(S_2COiPr)_3]_\infty$ under the same conditions. Thus, nature of the molecular architecture has been demonstrated to be important, at least for $Bi(S_2COR)_3$.

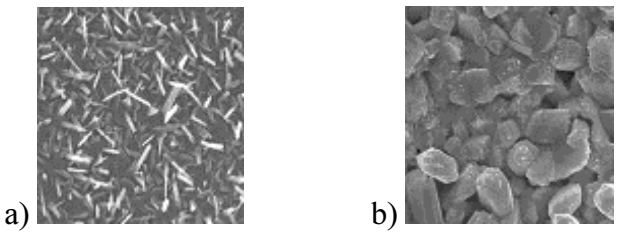

Figure 6. Scanning electron microscopy photographs of crystals of Bi_2S_3 obtained from the chemical vapor deposition method using (a) $[Bi(S_2COEt)_3]_2$ and (b) $[Bi(S_2COiPr)_3]_\infty$, as precursor materials. In (a), the nanorods are approximately 20 nm wide and 150 nm long. In (b), the crystals are approximately one micrometer in length.

Reflecting on the two structures shown in Figure 5, one realizes the structure with the largest R group, at least of those discussed here, adopts the structure with the greater aggregation, *i.e.* in contrast to the two systems described above in **2.1** and **2.2**. This theme is explored further in the following section.

2.4 Mercury xanthates

The mercury xanthates, $Hg(S_2COR)_2$, are known to adopt three distinct structural motifs. The first of these motifs for $Hg(S_2COR)_2$ is found for R = Me[20] and is shown in Figure 7(a). The mercury atom exists in a 3-coordinate, T-shaped geometry defined by a S_3 donor set. In this motif, a helical chain is formed owing to the presence of bidentate

bridging xanthate ligands. The remaining coordination site is occupied by a sulfur atom derived from a monodentate xanthate ligand. When the R group is changed to ethyl, a new motif, analogous to that found for $[Zn(S_2COEt)_2]_\infty$ is found;[21,22] see Figure 3(c). Thus, not only is a new motif found when the nature of R is altered but, a different coordination number. In the structure of $[Hg(S_2COiPr)_2]_\infty$[23] the 16-membered rings noted in the R = Et structure are still present but their mode of aggregation is quite distinct as can be seen from Figure 7(b). Two corners of the 16-membered ring are 'terminated' by chelating xanthate ligands. The two remaining corners have bridging xanthate ligands. For each of these mercury sites, one of the xanthate ligands extends laterally to link a neighboring 16-membered ring as for the R = Et motif. The two

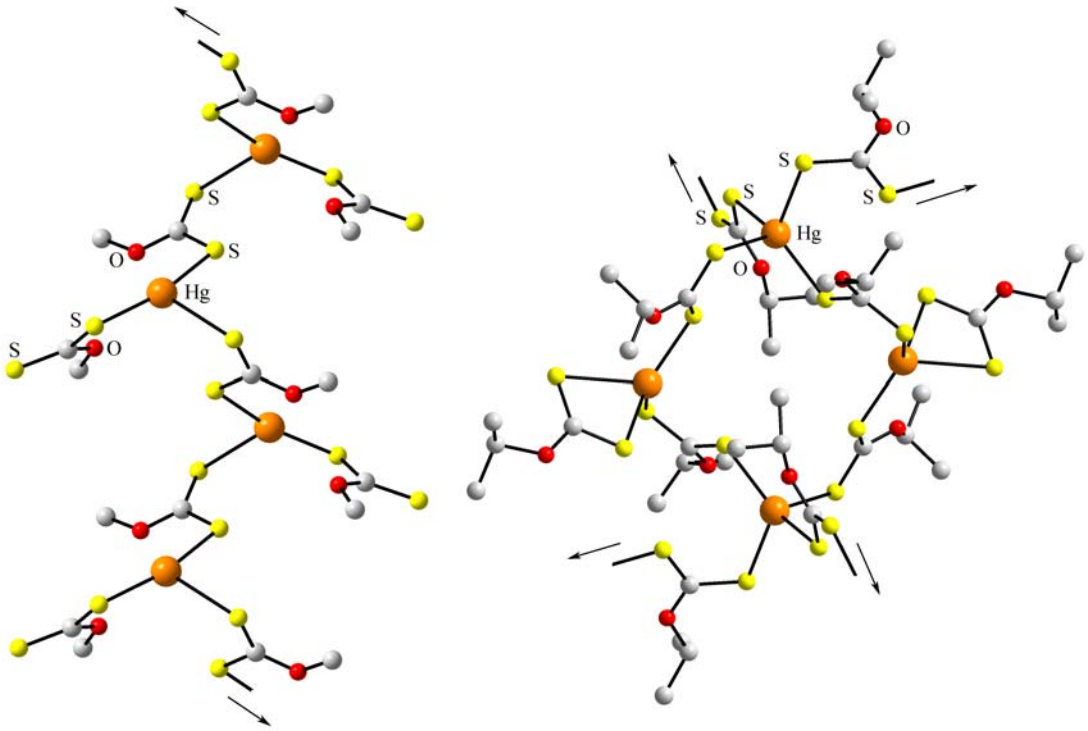

Figure 7. (a) The helical chain structure of $[Hg(S_2COMe)_2]_\infty$ with 3-coordinate mercury; and (b) The 3-dimensional or network structure of $[Hg(S_2COiPr)_2]_\infty$. Carbon-bound hydrogen atoms have been omitted for clarity.

remaining xanthate ligands project above and below the reference 16-membered ring to bridge different 16-membered rings. Such an arrangement leads to a 3-dimensional or

network structure. In the context of the previous discussion of the $R_3Sn(O_2CR')$ and $Zn(S_2COR)_2$ structures, the conclusions that there is a measure of steric control exerted by the tin- (**2.1**) or xanthate-bound R groups (**2.2**) over molecular aggregation does not hold true for the $Hg(S_2COR)_2$ structures, where it appears that an inverse correlation between the degree of molecular aggregation and the steric profile of the xanthate-bound R groups exists.

Quite plainly, global crystal packing considerations must be taken into account when rationalizing the appearance of different structural motifs, a task that is far from being straightforward. In order to demonstrate that crystal engineering is indeed feasible and to avoid finishing this discourse off on a disappointing note, a successful adventure in crystal engineering will be described.

3. Tuning aurophilic interactions in phosphinegold(I) thiolates

In this final section, a description of the manipulation of hydrogen bonding interactions so as to allow for the formation of aurophilic (*i.e.* Au…Au) interactions is described. Studies on the control of intermolecular aggregation in phosphinegold(I) thiolates are of interest as these compounds have applications as luminescent materials and therefore are of some practical importance.[24] The system to be described is based on the chemical structure shown in Scheme 3. Basically, the molecule is constructed about a ferrocene entity that has been symmetrically substituted by two diphenylphosphine groups. These in turn coordinate gold(I) thiolate residues that differ in their hydrogen-bonding functionality.[25]

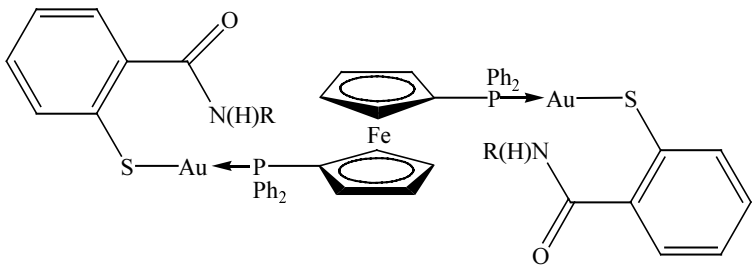

Scheme 3. The chemical structure of the repeat unit in $\{[Au(SC_6H_4C(=O)N(R)H-2)]_2(dppf)\}_\infty$, where R = H or Me.[25]

In the structure where R = H, illustrated in Figure 8(a), a polymeric array is found mediated by hydrogen-bonding interactions between the amide groups as well as aurophilic interactions. The amide-H atom not participating in the hydrogen-bonded amide-dimer, forms an interaction with the coordinated sulfur atom (not shown in the Figure). A similar structural motif is found in the structure where R = Me, *i.e.* where the hydrogen-bonding potential has been reduced somewhat. So, whereas a polymeric structure has again been generated, this is mediated solely by aurophilic interactions; see Figure 8(b). In this case, the amide-H forms an intramolecular interaction to the

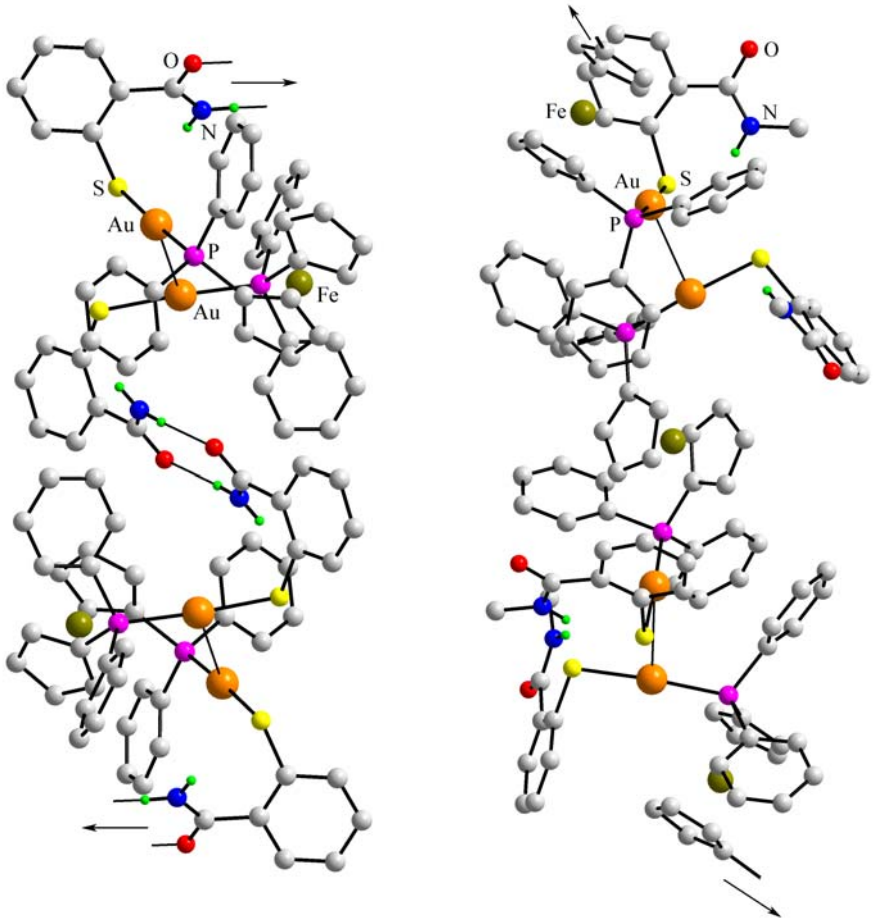

(a) (b)

Figure 8. (a) The polymeric structure of {[Au($SC_6H_4C(=O)NH_2$-2)]2(dppf)}$_\infty$; (b) The polymeric structure of {[Au($SC_6H_4C(=O)N(Me)H$-2)]2(dppf)}$_\infty$. Carbon-bound hydrogen atoms have been omitted for clarity.[25]

coordinated sulfur atom. As would be anticipated, the magnitude of the aurophilic interactions, at least as judged by the Au…Au separation, is stronger in the latter structure (2.9923(10) Å) compared with the former (3.2555(4) Å). Interestingly, the compactness of the polymeric chains, as measured by the separation between gold atoms in successive repeat units, is effectively the same at 11.2 Å in the latter and 10.7 Å in the former structure. Thus, the additional hydrogen-bonding interactions in the former structure have a relatively minor influence upon the coherence of the polymeric structure. This key result points to the potential utility of aurophilic interactions as a structure-directing tool.

4. Conclusions

From the foregoing discussion, several conclusions may be drawn. Perhaps the most obvious is the potential of steric control, whether metal- or ligand-based, over the aggregation of individual molecules in the solid state. This might be a tool that may prove useful in the design of molecular assemblies. The influence of precursor structure upon materials generation has been demonstrated in at least one of the systems described. This gives future work in this area relevance in materials chemistry and provides further impetus for on-going investigations. For the researcher, the undeniable 'take-home message' is the power of systematic structure analyses. The rewards are great! In these days where other avenues for structure determination exist in the absence of 'suitable' crystals for conventional X-ray crystallography, such as synchrotron radiation sources and powder diffraction methods, investigations of this type are sure to provide most useful information as to the nature of the solid state/crystal packing.

Acknowledgements

On-going work in gold (R-143-000-139-112), main group element thiolate (R-143-000-151-112) and organotin (R-143-000-186-112) chemistry is supported by the National University of Singapore.

References and Notes

1. http://pubs.acs.org/journals/cgdefu/index.html.
2. http://www.rsc.org/is/journals/current/crystengcomm/cecpub.htm.
3. http://www.elsevier.com/locate/issn/14630184.
4. A. G. Davies, Organotin Chemistry. V.C.H., Weinheim, Germany, 2nd Edition (1997).

5. P. J. Smith, Editor. Chemistry of Tin. Blackie Academic & Professional, London, England, 2nd Edition (1998).
6. E. R. T. Tiekink, *Appl. Organomet. Chem*. **1991**, *5*, 1–23.
7. E. R. T. Tiekink, *Trends Organomet. Chem*. **1994**, *1*, 71–116.
8. R. Willem, I. Verbruggen, M. Gielen, M. Biesemans, B. Mahieu, T. S. Basu Baul, and E. R. T. Tiekink, *Organometallics* **1998**, *17*, 5758–5766.
9. S. W. Ng, C. Wei, and V. G. Kumar Das, *J. Organomet. Chem*. **1988**, *345*, 59–64.
10. T. Ito, *Acta Crystallogr*. **1972**, *B28*, 1697–1704.
11. T. Ikeda and H. Hagihara, *Acta Crystallogr*. **1966**, *21*, 919–927.
12. C. S. Lai, Y. Z. Lim, T. C. Yap, and E. R. T. Tiekink, *Crys. TEng. Comm.* **2002**, *4*, 596–600.
13. M. J. Cox and E. R. T. Tiekink, *Z. Kristallogr*. **1999**, *214*, 242–250.
14. M. J. Cox and E. R. T. Tiekink, *Z. Kristallogr*. **1999**, *214*, 584–590.
15. M. A. Buntine, M. J. Cox, Y. X. Lim, T. C. Yap, and E. R. T. Tiekink, *Z. Kristallogr*., **2003**, *218*, 56–61.
16. M. R. Snow and E. R. T. Tiekink, *Aust. J. Chem*. **1987**, *40*, 743–750.
17. E. R. T. Tiekink, *Main Group Metal Chem*. **1994**, *17*, 727–736.
18. B. F. Hoskins, E. R. T. Tiekink, and G. Winter, *Inorg. Chim. Acta* **1985**, *99*, 177–182.
19. Y. W. Koh, C. S. Lai, A. Y. Du, E. R. T. Tiekink, and K. P. Loh, *Chem. Mat*., submitted.
20. E. R. T. Tiekink, *Acta Crystallogr*. **1987**, *C43*, 448–450.
21. Y. Watanabe, *Acta Crystallogr*. **1977**, *B33*, 3566–3568.
22. C. Chieh and K. J. Moynihan, *Acta Crystallogr*. **1980**, *B36*, 1367–1371.
23. Y. Watanabe, *Acta Crystallogr*. **1981**, *B37*, 553–556.
24. H. Schimdbaur, *Nature (London)* **2001**, *413*, 31–33.
25. D. R. Smyth, J. Hester, V. G. Young Jr, and E. R. T. Tiekink, *Cryst. Eng. Comm.* **2002**, *4*, 517–521.

Povzetek

Podan je sistematičen strukturni pregled štirih sistemov: organokositrovih karboksilatov, R_3SnO_2CR', cinkovih in živosrebrovih ksantatov, $A(S_2COR)_2$, (A=Zn, Hg), ter bismutovih ksantatov, $Bi(S_2COR)_3$. Njihova strukturna raznolikost se odraža tako v koordinacijskem številu kot tudi v razporeditvi ligandov okrog centralnega atoma. Strukturne razlike v sistemih R_3SnO_2CR' in $Zn(S_2COR)_2$ so povezane z naravo organske skupine R, ki je del liganda v primeru cinkovih spojin oziroma je vezana direktno na kositer v primeru spojin R_3SnO_2CR'. Tako se ponuja nov koncept načrtovanja zgradbe kristalov: sterična kontrola nad agregacijo molekul. Vendar pa je strukturna analiza $Hg(S_2COR)_2$ pokazala, da koncept sterične kontrole ni univerzalen in ga ni možno vedno uporabiti. Strukturni motivi v primeru bismutovih ksantatov $Bi(S_2COR)_3$ se odražajo v različni strukturi nanodelcev tankih filmov Bi_2S_3, pri čemer so bili kot prekurzorji pri nastanku uporabljeni različni bizmutovi ksantati. Podana sta tudi primera dveh sistemov, koder vlogo pri nastanku polimera igrajo neobičajne intermolekularne Au···Au interakcije.